

FLORIDA STATE UNIVERSITY
COLLEGE OF ARTS AND SCIENCES

INVESTIGATING THE CAUSAL EVIDENCE
OF INTEGRATION BETWEEN COGNITIVE
CONTROL SYSTEMS

By

JESSICA WOOD

A Thesis submitted to the
Department of Psychology
in partial fulfillment of the
requirements for the degree of
Master of Science

2023

Jessica Wood defended this thesis on August 16, 2023.

The members of the supervisory committee were:

Derek E. Nee
Professor Directing Thesis

Caterina Gratton
Committee Member

Wen Li
Committee Member

The Graduate School has verified and approved the above-named committee members, and certifies that the thesis has been approved in accordance with university requirements.

TABLE OF CONTENTS

List of Tables	iv
List of Figures	v
Abstract	vi
1. INTRODUCTION	1
2. METHODS	5
2.1 Participants and Procedure	5
2.2 Task	6
2.3 MRI Acquisition	8
2.4 TMS Motor Thresholding	8
2.5 cTBS Procedure	9
2.6 Target E-field Modeling	9
2.7 Image Preprocessing	9
2.8 Preprocessing of B_0 Inhomogeneity Mappings	10
2.9 Anatomical Data Preprocessing	10
2.10 Functional Data Preprocessing	10
2.11 Univariate Image Analysis	12
2.12 Functional Connectivity	13
2.13 ROI Analysis	13
2.14 Whole-Brain Network Analysis	14
3. RESULTS	15
3.1 ROI Analysis	15
3.2 Whole-Brain Network Analysis	17
4. DISCUSSION	21
APPENDICES	24
A. IRB HUMAN SUBJECTS APPROVAL LETTER	24
B. STUDY PERSONNEL	27
C. BEHAVIORAL CONSENT FORM	28
D. FUNCTIONAL MAGNETIC RESONANCE IMAGING CONSENT FORM	34
E. TRANSCRANIAL MAGNETIC STIMULATION CONSENT FORM	43
References	51
Biographical Sketch	56

LIST OF TABLES

Table 1. ROI Coordinates	14
--------------------------------	----

PREVIEW

LIST OF FIGURES

Figure 1. Model of Segregation and Integration based on Effective Connectivity.....	3
Figure 2. Comprehensive Control Task.....	4
Figure 3. Study Timeline.....	6
Figure 4. cTBS Target Localization.....	9
Figure 5. Baseline Functional Connectivity Within- and Between-Systems.....	16
Figure 6. Within-System Functional Connectivity across Visits.....	17
Figure 7. Between-System Functional Connectivity across Visits.....	17
Figure 8. Whole-Brain Network Connectivity at Baseline.....	18
Figure 9. Effect of Time vs Target in DMN Connectivity.....	19

ABSTRACT

Cognitive control is an imperative human function that allows one to behave in flexible manners when habit will not suffice. The neural mechanisms and interactions of the activated brain regions underlying cognitive control are not fully understood. Prior work has focused on the frontoparietal control network (FPCN) as the network responsible for executing the goal-oriented behaviors necessary for enacting control. Evidence shows that within the FPCN are three separable control subsystems, the temporal control (TC), contextual control (CC), and sensory-motor control (SC) systems. These systems are organized along a somatomotor-distal to somatomotor-proximal axis and involved in future- to present-oriented behavior (Nee, 2021). Prior research using effective connectivity between these systems suggested that the CC system is responsible for integration within the FPCN, whereas the TC and SC systems remain segregated. Underscoring the importance of such integration, an index of integration was found to be predictive of broad cognitive ability (Nee, 2021). Based on the roles of the control demand systems, integration therefore may be a key characteristic of control to connect plans with action execution.

To further test this model with measured brain signals, the current study used continuous theta-burst transcranial magnetic stimulation (cTBS) to causally contrast two regions within the TC system and a control site. Based on the TC system's segregative profile, we predicted that disrupting regions in the TC system would lead to increased integration amongst the control systems. Integration was assessed via functional connectivity of the functional magnetic resonance imaging (fMRI) blood-oxygenation level dependent (BOLD) signal assessed immediately following cTBS. In contrast to our predictions, we did not find any statistically significant changes in functional connectivity when comparing cTBS targets. Further analyses probed the within- and between-network connectivity of large-scale networks related to cognitive control. These analyses also demonstrated no statistically significant evidence for changes caused by cTBS. These results and implications for the findings are discussed.

CHAPTER 1

INTRODUCTION

Humans have an exceptional ability to flexibly behave in goal-oriented manners amongst ever-changing environments. This flexibility is underpinned by cognitive control which selects non-automatized actions. Though critical for higher-level cognitive functioning, the neural mechanisms underlying cognitive control remain elusive. Cognitive control engages a constellation of brain areas, most of which are represented in the frontoparietal control network (FPCN, (Dosenbach et al., 2008; Seeley et al., 2007; Yeo et al., 2011)). Recent work has demonstrated that the FPCN can be organized by an external-internal functional gradient along a somatomotor-proximal to somatomotor-distal axis (Dixon, 2018; Murphy et al., 2020; Nee, 2021). Nee (2021) decomposed the gradient into three control demand subsystems, wherein somatomotor-proximal regions link action to stimuli subserving an external and present-oriented form of control referred to as sensory-motor control (SC). Somatomotor-distal regions subserve internal and future-oriented control, or temporal control (TC), used for planning and future-oriented goals. Intermediate regions of the gradient subserve contextual control (CC), enabling context-appropriate behaviors informed by both present demands and future goals. This neural pattern provides insight about the functional organization of the FPCN, but leaves open how control demand subsystems interact to produce flexible behavior.

To detail interactions among control demand subsystems, previous work has modeled effective connectivity, which refers to the directional influence of brain areas towards one another (Nee, 2021; Nee & D'Esposito, 2016, 2017). Nee (2021) detailed that while effective influences among areas within the TC subsystem were positive, influences from the TC subsystem to CC and SC subsystems were negative. This author posited that such a pattern may serve to segregate the processing of the TC subsystem from other subsystems, facilitating future-oriented control at the expense of present-oriented control (Nee, 2021). Comparatively, the CC subsystem showed widespread positive connectivity across the networks, displaying an integration profile that may facilitate producing context-appropriate behaviors informed by both present demands and future goals (summarized schematic in Figure 1). Underscoring the importance of such integration, an index of integration was found to be predictive of broad cognitive ability (Nee, 2021). Based on

the roles of the control demand systems, integration therefore may be a key characteristic of control to connect plans with action execution.

While these results are intriguing, effective connectivity was derived from generative modeling (Friston et al., 2003). Such approaches can be successful only insofar as models can be properly identified. However, neural dynamics are highly complex, and non-invasive measurements in humans (e.g., fMRI) are noisy. Combined, this renders the problem of identifying a generative model of neural dynamics extremely difficult. Causal techniques to more directly determine the physiological dependence of areas upon another could substantially resolve the problem.

The present study employs transcranial magnetic stimulation (TMS) to examine the causal dependence of network interactions during a cognitive control task designed to manipulate the three proposed control demands (task summarized in Figure 2). Here, continuous theta burst stimulation (cTBS) was implemented to examine the effects of focal perturbation to the broader FPCN affording a direct means to detail the effective influences of perturbed areas onto other areas. As the effects of cTBS are putatively inhibitory (Huang et al., 2005), we hypothesized that stimulation to areas within the TC subsystem would disrupt its segregative influences. In turn, such disruption would be expected to increase integration among the control subsystems. To test these effects, we compared the correlated activation patterns, or functional connectivity, between the cTBS targets and each control demand subsystem (TC, CC, SC). In this case, functional rather than effective connectivity was employed as the former can be analytically computed directly from measured signals, avoiding any obscuring of the results by model identifiability issues. Functional connectivity among control demand subsystems was examined pre- and post-perturbation with the prediction that greater functional connectivity among subsystems will be observed post-perturbation, consistent with heightened integration.

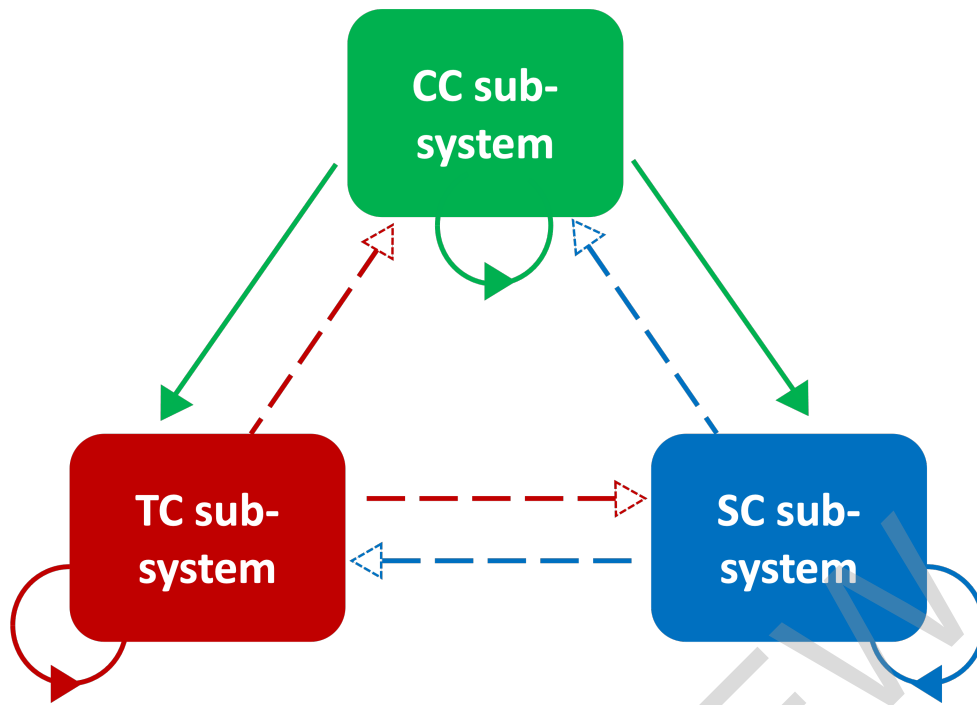


Figure 1. Model of Segregation and Integration based on Effective Connectivity. Schematic summarizing effective connectivity modeling results from Nee (2021). Each control demand system is shown: Temporal Control (TC; red), Contextual Control (CC; green), and Sensory-motor Control (SC; blue). Excitatory/positive connections are demonstrated by solid lines and inhibitory/negative connections are demonstrated by dashed lines. Results demonstrated positive within-network effective connectivity in all control demand systems (small, within-system recurrent circles). Positive between-network effective connectivity was only demonstrated in the CC network, showing integration between control subnetworks. TC (red) and SC (blue) showed negative between-network connectivity, segregating processing.

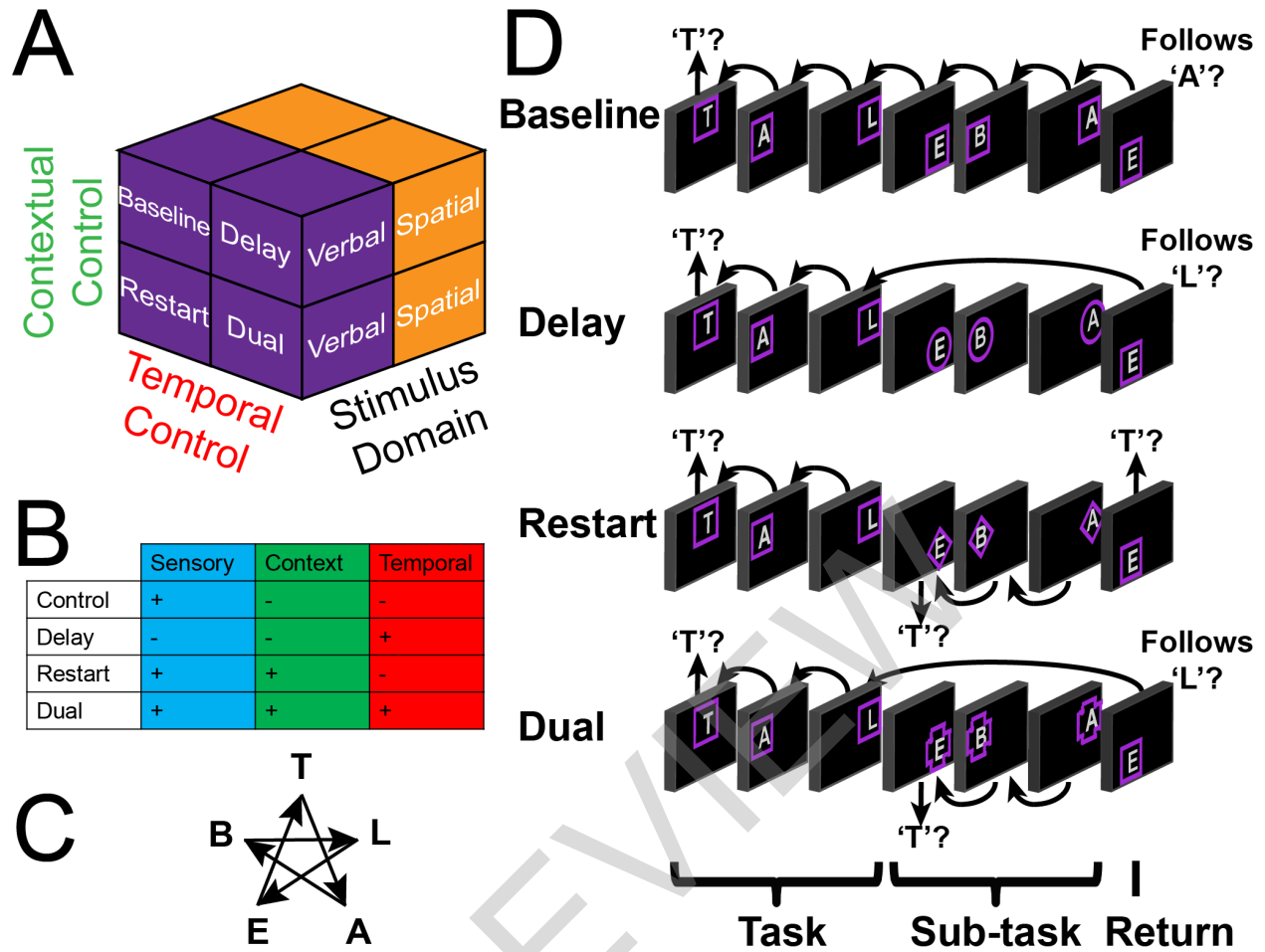


Figure 2. Comprehensive Control Task. A-B) Visualization of the 2 x 2 x 2 factorial design of the CCT. C) Participants learned both verbal sequence (TABLET) and spatial sequence (points of a star) domains. D) Example blocks of each condition (shown across one consistent stimulus domain). Adapted from Nee & D'Esposito, 2016.

CHAPTER 2

METHODS

2.1 Participants and Procedure

This study recruited 60 participants. 26 participants were dropped from the experiment (4 due to low task accuracy, 3 due to claustrophobia inside the MRI scanner, 6 due to other MRI intolerance, 1 due to an adverse event, and 12 due to scheduling and/or other personal removal from the study). This resulted in 34 participants that completed the total 5-session experiment, including 23 females and 11 males with an average age of 19.41 (range 18-25). Participants were screened for all MRI, TMS, and computer task requirements. Participants were required to be fluent in English by age 6, right-handed, and have no previous history of neurological or current psychiatric disorders.

Figure 3 shows the timeline of the study sessions. During Visit 1, participants were trained on the task until proficient - by averaging 85% across all trials. Participants that were unable to achieve 85% accuracy were removed from the study. Within one week of Visit 1, participants completed Visit-2 including 6 runs of the task within the scanner followed by TMS motor thresholding (see details below). Visits 3, 4, and 5 included cTBS to a randomized and counterbalanced target (middle frontal gyrus – MFG, lateral frontal pole – FPI, or primary somatosensory cortex – S1), followed by 4 runs of the task within the scanner. Participants were paid and completed informed consent consistent with the Florida State University Institutional Review Board.

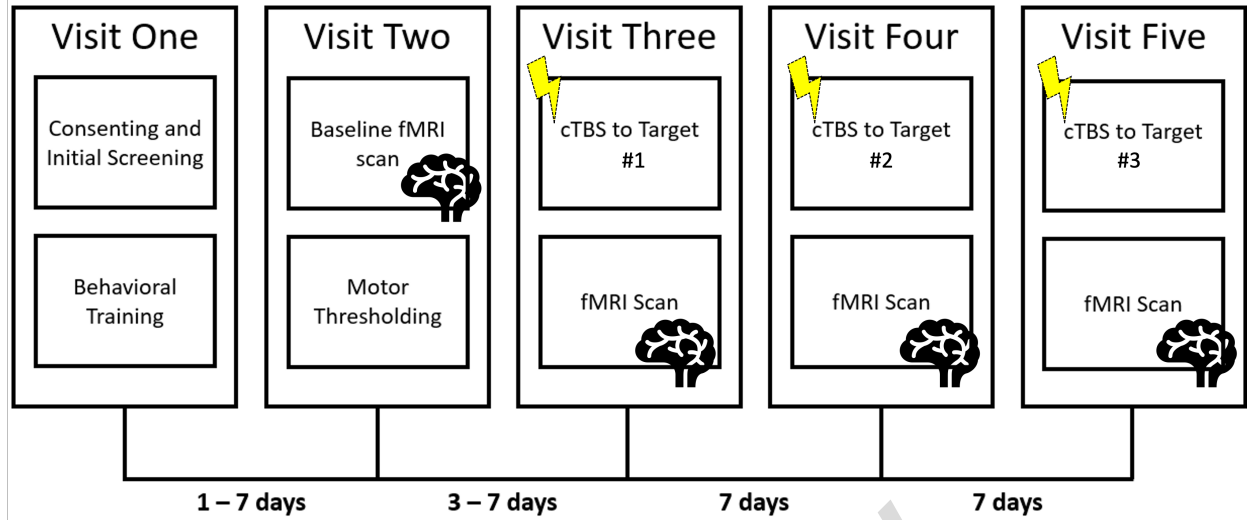


Figure 3. Study Timeline. Subjects completed a 5-day experiment with behavioral training completed on Visit One, a baseline fMRI scan for task and TMS target localization on Visit Two, and once per week completed a cTBS session with randomized targets followed by an fMRI scan.

2.2 Task

The Comprehensive Control Task (CCT) was first described in Nee & D’Esposito (2016), and originally modified from previous work (Charron & Koechlin, 2010; Koechlin et al., 1999). The task is a 2 x 2 x 2 factorial design with levels of TC (high, low), CC (high, low), and stimulus domain (verbal, spatial) (Figure 2). Across the first two factors of control are four conditions (displayed in both verbal and spatial domains): 1. Baseline, 2. Restart, 3. Delay, 4. Dual. The foundation of the task is built around the baseline condition which tests the primary stimulus-response mappings inherent in SC. In this condition, participants are taught the sequence T-A-B-L-E-T (verbal domain) and the sequence of the 5-points of a star (spatial domain). Stimuli are letters in one of 5 screen locations, cued by a surrounding shape. The square shape is constant across participants as the baseline condition shape, and the color of the shape cues the participant to begin either the spatial or verbal task. The basic task is to respond yes or no, mapped onto a left- or right-button response, determining whether the letter/position is the beginning of the sequence (e.g., “T” for verbal or the top-center position for spatial). The following trials require the participant to determine whether the current stimulus follows the prior stimulus within the sequence (e.g., “A” follows “T” in the verbal sequence). All other conditions begin and end with this baseline task, and add task demands cued by a shape-change during the subtask phase of a block. In the restart condition, the shape-change cues the participant to restart the baseline task,

i.e., regardless of where they were in the baseline task, determine whether the current stimulus is the beginning of the sequence. Participants then continue the baseline task until a shape-change occurs again, to which they restart the task once more. This condition adds in CC demands by engaging multiple task-sets during the subtask phase, requiring the participant to adapt their behavior based on rules. In the delay condition, the shape-change cues the participant to keep in mind the previous stimulus to be used on a future trial, while ignoring each new stimulus by responding “no” to all stimuli. Upon a shape-change back to the baseline task (the ‘return’ trial), participants determine whether the stimulus follows the previously held-in-mind stimulus from before the “ignore” trials. This task adds in TC demands during the subtask, which require future-oriented planning based on the item to-be-remembered for the return trial. Finally, the dual task includes a shape-change that combines the restart and delay rules, i.e., determining whether the stimulus is the beginning of the sequence, while also keeping the previous stimulus in mind for a future trial. Participants subsequently continue with the baseline task until the shape-change cues the participant to determine whether the new stimulus followed the held-in-mind stimulus from the previous shape-change. Based on this combination of conditions, the dual task engages TC, CC, and SC demands within the subtask phase. Shape-cues for each condition, shape-color cues for stimulus domain, and left-right response mappings were randomized and counter-balanced across participants.

The subtask phases were designed to factorially vary the control demands, TC (high = delay and dual, low = baseline and restart), and CC (high = restart and dual, low = baseline and delay), across both stimulus domains (verbal, spatial), resulting in a $2 \times 2 \times 2$ design. SC was also varied across conditions (high = baseline, restart, and dual, low = delay). This results in distinct contrasts of each control demand while marginalizing over stimulus domain: main effect of TC = (dual + delay) – (restart + baseline); main effect of CC = (dual + restart) – (delay + baseline); and SC = (dual + baseline) – (restart + delay). The SC contrast is effectively the interaction term of the TC and CC factors.

Participants were trained by a study assistant through guided practice, and then completed 2 runs of the task independently. Participants were required to reach 85% accuracy by the end of the 2 runs, otherwise, they were compensated and dismissed from participating further. In the

baseline fMRI Visit-2, participants completed 6 runs within the scanner. In each cTBS Visit (3-5) participants completed 4 runs, totaling 18 runs per participant. Within each run, there were 16 blocks consisting of 7-11 trials: 2-3 first baseline trials, 3-5 subtask trials, and 2-3 second baseline trials. This resulted in 9 minute and 38 second task runs, for a total of approximately 173 minutes of task data per participant, before preprocessing.

2.3 MRI Acquisition

Images were acquired on a 3T Siemens Prisma scanner equipped with a 32-channel head coil located in the MRI Facility at Florida State University. Stimuli were presented to the participant via a coil-attached mirror reflecting a projector situated at the bore of the magnet. Experimental tasks were presented using MATLAB software version R2020a. Eye position was gathered using an EyeLink 1000 eye tracker and monitored for participant vigilance (SR Research, Inc.). Response data were collected on an MR-compatible button box (Current Designs, Inc.). T2*-weighted images were acquired using an EPI sequence with 35 descending slices and $3.4375 \times 3.4375 \times 3.8 \text{ mm}^3$ voxels (TR = 2000 ms; echo time = 25 ms; flip angle = 70; field of view = 220 mm). Dummy acquisitions preceded each run to allow for image stabilization. Phase and magnitude images were collected to estimate the magnetic inhomogeneity. High-resolution T1-weighted MPRAGE images were collected for spatial normalization and anatomic localization ($0.7 \times 0.7 \times 0.7 \text{ mm}^3$ isotropic voxels; TR = 1840 ms; echo time = 2.9 ms; flip angle = 9).

2.4 TMS Motor Thresholding

TMS was conducted using a MagVenture MCF-B65 SLS stimulator equipped with a 75mm diameter figure-eight coil. Electromyography (EMG) was recorded using electrodes placed on the first dorsal interosseus (FDI) muscle on the left hand. First, a 'hunting procedure' was used to determine the scalp location in the right hemisphere producing the maximal contralateral index finger contraction at the minimal stimulation intensity. Upon localization of the motor cortex, the participant was asked to maintain voluntary contraction of the FDI muscle at ~20% of maximum contraction. Active motor threshold (AMT) was determined as the minimal stimulation intensity needed to produce a motor-evoked potential in 5 out of 10 pulses.